ISSN 1547-4771, Physics of Particles and Nuclei Letters, 2008, Vol. 5, No. 3, pp. 243–247. © Pleiades Publishing, Ltd., 2008.

Minimalistic Hybrid Models for the Adsorption of Polymers and Peptides to Solid Substrates[1]

M. Bachmann and W. Janke

Institut für Theoretische Physik and Centre for Theoretical Sciences (NTZ), Universität Leipzig, 04009 Leipzig, Germany
e-mail: {bachmann,janke}@itp.uni-leipzig.de

Abstract—We have performed chain-growth simulations of minimalistic hybrid lattice models for polymers interacting with interfaces of attractive solid substrates in order to gain insights into the conformational transitions of the polymers in the adsorption process. Primarily focusing on the dependence of the conformational behavior on temperature and solubility, we obtained pseudophase diagrams with a detailed structure of conformational subphases. In the study of hydrophobic-polar peptides in the vicinity of different types of substrates, we found a noticeable substrate specificity of the assembly of hydrophobic domains in the conformations dominating the adsorption subphases.

PACS numbers: 02.70.Ns; 87.15.–v

DOI: 10.1134/S1547477108030229

INTRODUCTION

Understanding molecular self-assembly at organic–inorganic interfaces is essential for the design of related future nanotechnological applications, e.g., microscopic sensory devices in biomedicine and nanoelectronic circuits. Recently, the enormous progress in the development of high-resolution equipment allowed experiments which revealed quite interesting properties of such hybrid interfaces as, e.g., the specific dependence of peptide adhesion to the type of attractive substrates and peptide sequences [1–3]. In studies of short peptides consisting of 12 amino acids, it was found, e.g., that the adhesion strength to a (100) silicon (Si) surface improved by a factor of about 15 only by permuting the order of amino acids in this sequence. On the other hand, the adsorption strengths of the same sequences to gallium arsenide (GaAs) with (100) orientation hardly differ [2]. The reasons for this binding specificity are not yet understood and an appropriate atomic model explaining the specific substrate–peptide cooperativity on the microscopic scale is still lacking. This problem is related to similar studies where the adsorption and docking behavior of polymers is essential, e.g., protein–ligand binding [4], prewetting and layering transitions in polymer solutions, as well as dewetting of polymer films [5], molecular pattern, electrophoretic polymer deposition, and growth [6].

CONFORMATIONAL TRANSITIONS ACCOMPANYING HOMOPOLYMER ADHESION

For the following study of the conformational behavior of a homopolymer in the adsorption process to a solid, attractive substrate, we employ a strongly simplified coarse-grained model. The homopolymer is modeled as an interacting self-avoiding walk on a simple cubic (sc) lattice in implicit solvent, and the energy of a given conformation is related to the number n_m of nearest-neighbor contacts of monomers being nonadjacent along the chain. In the adsorption phase, the surface contact energy in our model is proportional to the number of monomers in the surface-contacting layer, and the number of monomer-substrate contacts is denoted as n_s. Introducing an overall energy scale ε_0 (which is set to unity in the following) and a parameter s that rates the energy scales of the polymer conformation and the surface contact energy, the minimalistic model is written as [7–9]:

$$E_s(n_s, n_m) = -\varepsilon_0(n_s + sn_m). \qquad (1)$$

Since the parameter s effectively controls the compactness of the polymer conformations, it can also be interpreted as kind of solubility (the larger the value of s, the worse the quality of the solvent). In our simulations, we applied the contact-density chain-growth method, which is a generalized variant of the multicanonical chain-growth algorithm [10]. This method allows a precise estimation of the contact density $g(n_s, n_m)$, which is the number of conformations with n_s surface and n_m intrinsic contacts. For the homopolymer with 179 monomers used in our study, $g(n_s, n_m)$ ranges over more than 120 orders of magnitude, as shown in Fig. 1.

The main advantage of directly sampling $g(n_s, n_m)$ in our simulation is that this quantity is independent of the external parameters temperature T and solubility s. This means, the calculation of energetic statistical quantities can be performed after the simulation for arbitrary values of T and s. Defining the partition sum by $Z =$

---

[1] The text was submitted by the authors in English.

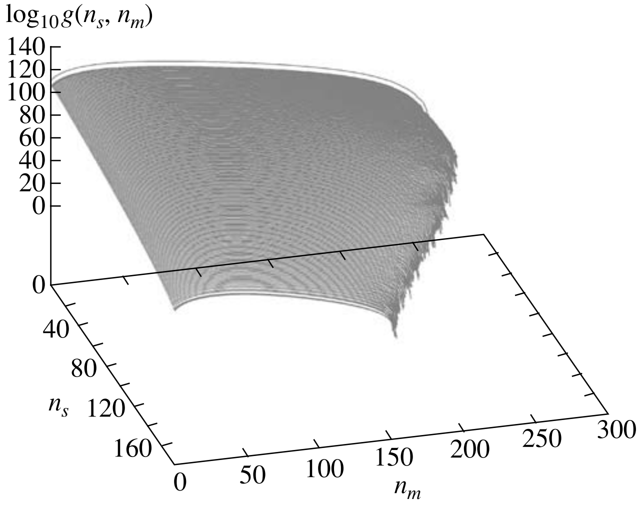

Fig. 1. Contact density $g(n_s, n_m)$ of a homopolymer with 179 monomers in a cavity with attractive substrate. For regularizing the number of unbound conformations (i.e., $n_s = 0$), a steric wall parallel to the attractive substrate was placed in a distance of $z_w = 200$ lattice units.

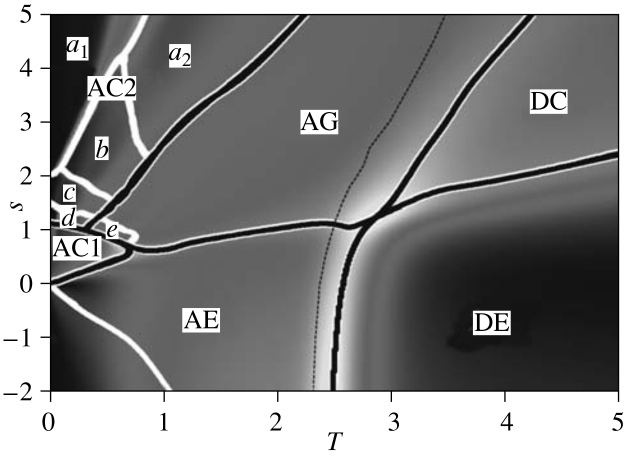

Fig. 2. Profile of the specific heat as a function of temperature T and solubility s. Black and white lines emphasize pseudophase transitions (cf. text). The dashed black line indicates the positions, where the free-energy minima of adsorbed and desorbed phases are degenerate, i.e., where both phases coexist with equal probability density.

$\sum_{n_s, n_m} g(n_s, n_m)\exp(-E_s/k_BT)$, ensemble averages of functions of the contact numbers $f(n_s, n_m)$ are obtained via $\langle f(n_s, n_m)\rangle = \sum_{n_s, n_m} f(n_s, n_m) g(n_s, n_m)\exp(-E_s/k_BT)/Z$. As our main interest is focused on the conformational transitions experienced by the polymer in the adsorption process, we consider in the following the specific heat, which is here a function of temperature and solubility: $C_V(T, s) = (\langle E_s^2\rangle - \langle E_s\rangle^2)/k_BT^2$. The profile of C_V is shown in Fig. 2, where bright regions highlight strong fluctuations, and black and white lines indicate conformational transitions. Black lines mark transitions that are assumed to resist the thermodynamic limit, whereas subphases specific to the precise length of the polymer are separated by white lines. The C_V profile can therefore also be interpreted as T–s pseudophase diagram of the hybrid system. There are two main regions, the desorption phases of respective compact and expanded conformations, DC and DE, and the phases of adsorbed conformations. The adsorption regime can be divided into compact filmlike (AC1) and layered (AC2*a*–*d*) phases, globular conformations with surface contact (AG, AG*e*), and extended conformations (AE). In the low-temperature and poor-solvent pseudophases AC1, AC2*a*–*d* and AG*e*, layered conformations dominate. In AC1 a two-dimensional, maximally compact polymer film is entirely in contact with the substrate. The less the influence of the solvent, the higher is the tendency of the polymer to form a maximum number of intrinsic contacts by forming layers. In AC2*d* and AG*e*, double-layer conformations dominate, in AC2*c* triple-layer, and in AC2*b* four-layer structures. The maximum number of intrinsic contacts in three dimensions is found in the five-layer structures in subphases AC2$a_{1,2}$. Note that trivial cubic symmetries are impossible as 179 is a prime number [8, 9].

SUBSTRATE SPECIFICITY OF PEPTIDE ADSORPTION

Considering peptides in the simplest representation, i.e., as a heteropolymer sequence of hydrophobic and polar residues on a simple cubic lattice, model (1), with slight modifications, can also be used to study peptide adhesion to substrates. In tertiary protein folding, the hydrophobic monomers form a compact core due to the hydrophobic effect, and the polar monomers screen this core from the aqueous environment. The two types of monomers naturally allow the investigation of three types of substrates: (a) the unspecifically attractive, (b) the hydrophobic, and (c) the polar substrate, where the latter two are only attractive to respective hydrophobic and polar monomers with surface contact. Therefore, model (1) is substituted by [11]:

$$E_s(n_s, n_{\mathrm{HH}}) = -\varepsilon_0(n_s + sn_{\mathrm{HH}}), \qquad (2)$$

where n_{HH} is the number of intrinsic nearest-neighbor contacts between nonadjacent hydrophobic monomers and n_s symbolizes the number of attractive surface contacts and thus depends on the type of substrate. In contact-density chain-growth simulations, we have studied the adsorption behavior of an exemplified heteropolymer of 103 monomers (66 polar, 37 hydrophobic), which is the hydrophobic-polar transcription of the amino acid sequence of *cytochrome c*. In Fig. 3, the specific heat profiles of the heteropolymer in the vicinity of the three different substrates are shown. Ridges (marked by white and gray lines) indicate conforma-

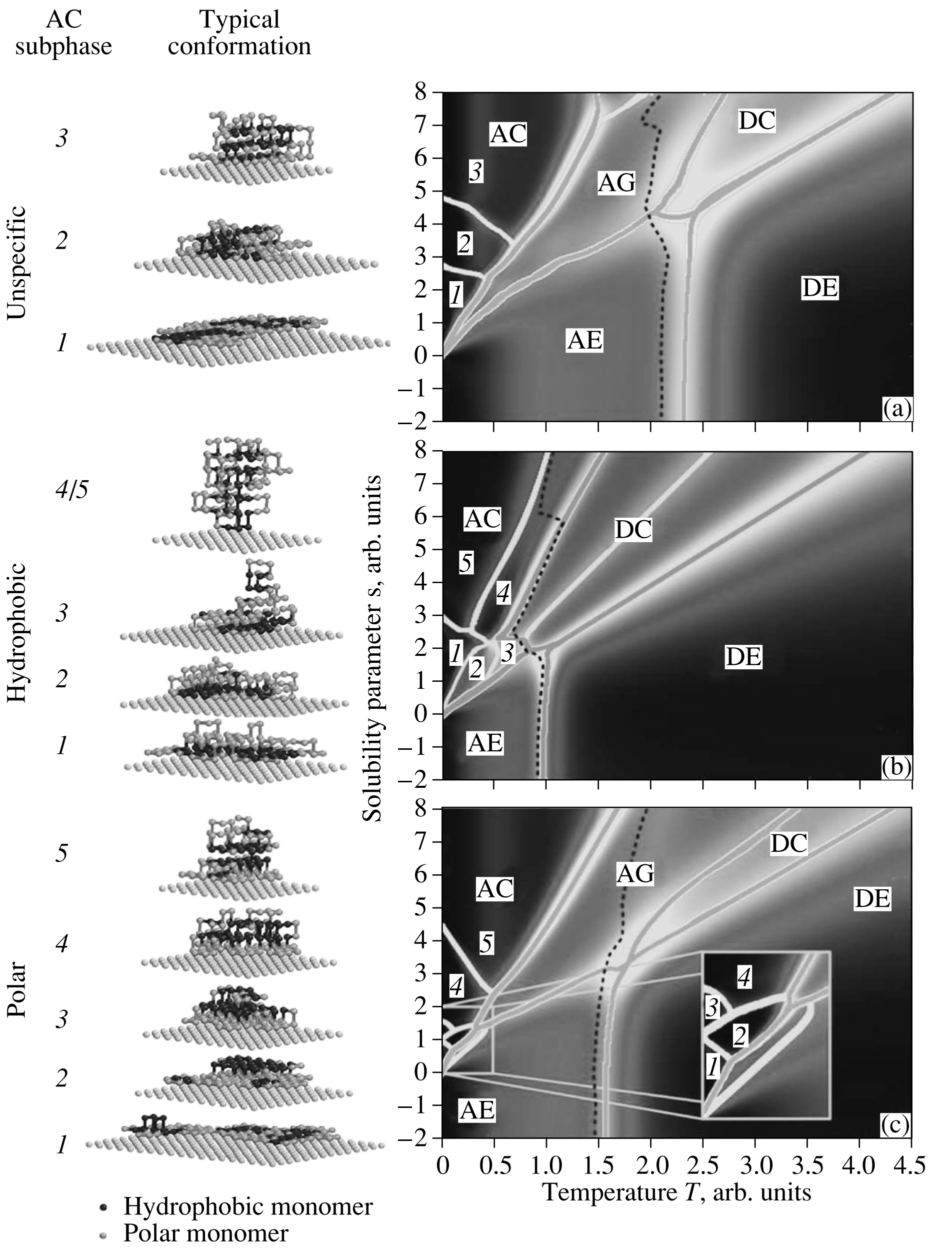

Fig. 3. Specific-heat profiles for substrates being (a) unspecifically attractive, (b) hydrophobic, and (c) polar. Also shown are typical conformations in the AC subphases.

tional pseudophase transitions. In the bulk phases, the typical expanded random-coil-like conformations (DE) and the compact, nativelike folds (DC) can be distinguished. In the adsorbed regime, we also find expanded (AE) and compact/globular (AC, AG) phases. Typical conformations in the fine-structured AC subphases are also shown in Fig. 3. The compactness of the hydrophobic domains in these subphases does not only depend on the solvent quality but also on the effect how polar residues hinder the formation of hydrophobic domains. On the hydrophobic substrate, there is an effective steric repulsion of the polar monomers, which are pushed off the surface layer. In the case of active attraction of polar residues to the polar substrate, the competing tendency of the hydrophobic monomers to form compact, layered clusters in poor solvent leads to the loss of surface contact of these cores.

An alternative glance at the phase behavior is thrown by exploring the free-energy landscape of the system. Considering the numbers of hydrophobic contacts n_{HH} and surface contacts n_s as natural system parameters, the free energy, expressed as function of these quantities, is defined as $F_{T,s}(n_s, n_{\mathrm{HH}}) = E_s(n_s, n_{\mathrm{HH}}) - TS(n_s, n_{\mathrm{HH}})$, where the "microcontact" entropy is related to the contact density $g(n_s, n_{\mathrm{HH}})$ via $S(n_s, n_{\mathrm{HH}}) =$

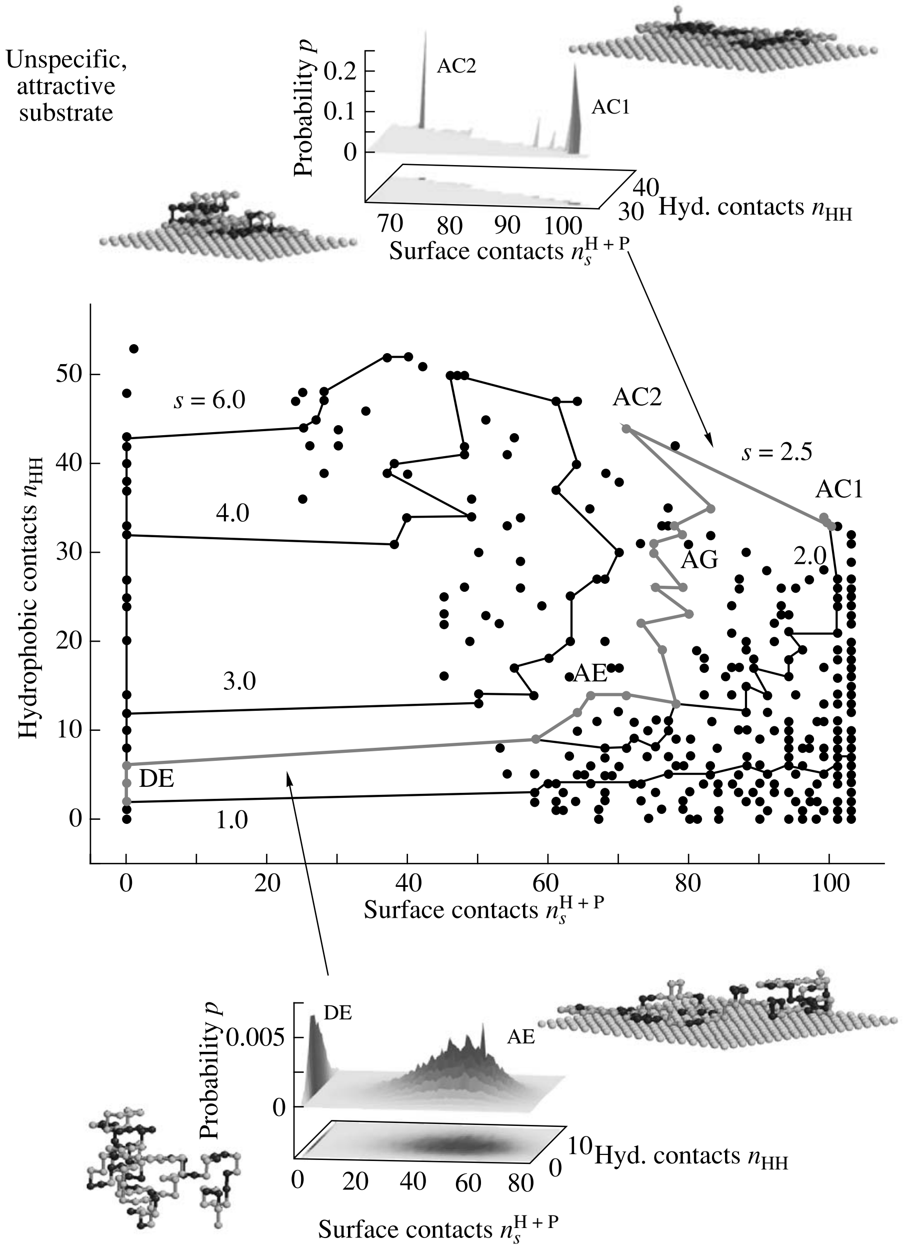

Fig. 4. Contact-number map of all free-energy minima for the 103-mer and substrate equally attractive to all monomers in the parameter space $T \in [0, 10]$, $s \in [-2, 10]$. Lines illustrate contact free energy changes with the temperature at constant solvent parameter s. For the exemplified solvent with $s = 2.5$, probability distributions close to the layering transition (AC1, 2) and the unbinding transition (AE to DE) are also shown.

$k_B \ln g(n_s, n_{HH})$. The minimum of $F_{T,s}(n_s, n_{HH})$ for given external parameters s and T is related to a class of macrostates with $n_s^{(0)}$ surface and $n_{HH}^{(0)}$ hydrophobic contacts which dominates the phase. In Fig. 4, we have plotted the map of *all* possible free-energy minima in the range of external parameters $T \in [0, 10]$ and $s \in [-2, 10]$ for the 103-mer in the vicinity of an unspecifically attractive substrate. Solid lines connect minima in the free-energy landscape when changing temperature under constant solvent (s = const) conditions. Following the exemplified trajectory for $s = 2.5$ and starting at very low temperatures, it is clear from Fig. 3a that the system resides in pseudophase AC1, i.e., compact, filmlike single-layer conformations dominate. The system obviously prefers surface contacts at the expense of hydrophobic contacts. Increasing the temperature, the system experiences close to $T \approx 0.35$ a first-order-like conformational transition, and a second layer forms (AC2). The loss of energetically favored substrate contacts of polar monomers is partly compensated by the energetic gain due to the more compact hydrophobic domains. Increasing the temperature further, globular, pancakelike conformations dominate in the globular pseudophase AG. Reaching AE, the number of hydrophobic contacts decreases further. Extended, dissolved conformations dominate. The transitions from AC2 to AE via AG are comparatively "smooth" (second-order-like), i.e., no immediate changes in the contact numbers passing the transition lines are noticed. The situation is different when approaching the unbinding transition line from AE close to $T \approx 2.14$. This transition is accompanied by a dramatic loss of substrate contacts—the peptide desorbs from the substrate. As the probability distribution in Fig. 4 shows, the unbinding transition looks again first-order-like, i.e., close to the transition line, there is a coexistence of adsorbed and desorbed conformations.

CONCLUSIONS

We have studied the conformational behavior of minimalistic hybrid interfaces of polymers and substrates and obtained from sophisticated chain-growth simulations pseudophase diagrams, which exhibit a rich pseudophase structure, in particular, in the adsorption regime. We could also show that the adsorption of heteropolymers is specifically dependent on the hydrophobic or polar character of the substrate. These results, whose experimental verification is still pending, are of particular interest for future applications of hybrid organic-inorganic materials in nanotechnology and biomedicine.

ACKNOWLEDGMENTS

This work is partially supported by a DFG (German Science Foundation) grant under contract no. JA 483/24-1. We thank the John von Neumann Institute for Computing (NIC), Forschungszentrum Jülich, for providing access to their supercomputer JUMP under grant no. hlz11.

REFERENCES

1. S. R. Whaley, D. S. English, E. L. Hu, P. F. Barbara, and A. M. Belcher, Nature **405**, 665 (2000).
2. K. Goede, P. Busch, and M. Grundmann, Nano Lett. **4**, 2115 (2004).
3. R. L. Willett, K. W. Baldwin, K. W. West, and L. N. Pfeiffer, Proc. Natl. Acad. Sci. (USA) **102**, 7817 (2005).
4. M. Ikeguchi, J. Ueno, M. Sato, and A. Kidera, Phys. Rev. Lett. **94**, 078102 (2005).
5. J. Forsman and C. E. Woodward, Phys. Rev. Lett. **94**, 118301 (2005).
6. G. M. Foo and R. B. Pandey, Phys. Rev. Lett. **80**, 3767 (1998).
7. T. Vrbová and S. G. Whittington, J. Phys. A **29**, 6253 (1996).
8. M. Bachmann and W. Janke, Phys. Rev. Lett. **95**, 058102 (2005).
9. M. Bachmann and W. Janke, Phys. Rev. E **73**, 041802 (2006).
10. M. Bachmann and W. Janke, Phys. Rev. Lett. **91**, 208105 (2003).
11. M. Bachmann and W. Janke, Phys. Rev. E **73**, 020901(R) (2006).